Characterization of optical and thermal distributions from an intracranial balloon applicator for photodynamic therapy

Steen J. Madsen*[a], Lars O. Svaasand[b], Bruce J. Tromberg[c] and Henry Hirschberg[d]

[a]Dept. of Health Physics, University of Nevada, Las Vegas, 4505 Maryland Pkwy., Box 453037, Las Vegas, NV 89154

[b]Norwegian University of Science and Technology, Trondheim, Norway

[c]Beckman Laser Institute and Medical Clinic, University of California, Irvine, CA 92715

[d]Dept. of Neurosurgery, Rikshospitalet, Oslo, Norway

ABSTRACT

An indwelling balloon applicator developed for postoperative intracavity brachytherapy was evaluated for photodynamic therapy. Measurements of light distributions in a brain phantom show that the applicator can be used to deliver sufficiently uniform light doses during PDT. The light distribution is uniform to within 5% when the balloon is filled with a scattering medium. Based on simple assumptions, it is shown that the applicator can be used to deliver a threshold optical dose to brain tissue at depths of 1.4 cm in less than 90 minutes. A mathematical model of the thermal distribution around the applicator suggests that tissue temperatures will be below the hyperthermic threshold at the input powers required for treatments to depths of 1.4 cm in the resection cavity. The delivery of threshold light doses to depths exceeding 1.4 cm is likely to result in hyperthermic effects to tissues near the applicator surface.

Keywords: Photodynamic therapy, balloon applicator, light distribution, thermal distribution, brain tumor

1. INTRODUCTION

The prognosis for patients with high grade gliomas has not improved significantly over the past four decades. Even with the best available treatments using surgery, radiation and chemotherapy, median survival is less than one year[1]. Although gliomas are considered to be disseminated tumors in the brain, most recur at the site of the previous tumor resection – approximately 80 % of tumors recur within 2 cm of the resected margin[2]. Improved local control would therefore be of clear benefit. Intracavity therapy offers the possibility of applying various treatment modalities (brachy, photodynamic and thermal therapies) aimed at the nests of tumor cells left in the resection border while minimizing damage to normal tissue[3-5].

Although photodynamic therapy (PDT) has been used in the treatment of brain tumors for the past 20 years[6], results of clinical trials have been ambiguous due, in part, to their limited scope. In almost all cases, PDT had been given single-shot, immediately following surgery. Due to the complicated nature of PDT dosimetry, there have been relatively few attempts to optimize PDT dose.

Delivery of sufficient light doses to tumor cells residing at cm depths in the resection cavity requires long treatment times due to the highly attenuating nature of brain tissue. Due to time limitations, the delivery of adequate light doses is not feasible using traditional one-shot intraoperative techniques. Furthermore, there is reason to believe that multi-fractionated PDT treatments over long time periods are more effective than one-shot procedures[7]. Protracted multi-fractionated PDT treatments are possible using indwelling balloon

- Correspondence: Email: steenm@ccmail.nevada.edu; Telephone: 702.895.1805; Fax: 702.895.4819

Laser-Tissue Interaction XII: Photochemical, Photothermal, and Photomechanical, Donald D. Duncan, Steven L. Jacques, Peter C. Johnson, Editors, Proceedings of SPIE Vol. 4257 (2001)

applicators such as the ones currently used in afterloading brachytherapy at the Rikshospital in Oslo, Norway[4].

The goals of this paper may be summarized as follows: (1) to determine the light distribution surrounding an indwelling balloon applicator to be used in postoperative PDT of malignant brain neoplasms; (2) to estimate typical treatment times based on very simple assumptions of light propagation in brain tissues, and; (3) to estimate thermal distributions in brain tissues during PDT.

2. THEORY

2.1. Optical distribution

In scattering media, such as biological tissue, the light distribution can be adequately described by diffusion theory. In the case of a spherical applicator positioned centrally in a spherical cavity, the fluence rate (W cm^{-2}) is given by[8]:

$$\varphi = \frac{\varphi_o e^{-r/\delta}}{r}, \tag{1}$$

where φ_o is the fluence rate at the inner surface of the cavity, r is the distance from the center of the cavity, and δ is the optical penetration depth.

Multiple reflections will build up the fluence rate in the cavity until the radiation transmitted through the cavity wall is equal to the light coupled into the cavity – the so-called integrating sphere effect. It is important to account for this effect as it reduces treatment times due to the fluence build-up. Furthermore, in a true integrating sphere effect, the irradiance is independent of source position in the applicator[9]. In the presence of the integrating sphere effect, the fluence rate is given by[8]:

$$\varphi = \left[\frac{P_t c}{4\pi a D r \left(\frac{1}{a} + \frac{1}{\delta} \right)} \right] e^{-(r-a)/\delta}, \tag{2}$$

where P_t is the total optical power from the applicator, c is the velocity of light in tissue, a is the radius of the spherical cavity, and D is the diffusion constant. The total optical dose (Ψ) at a particular depth is given by:

$$\Psi = \varphi \cdot t, \tag{3}$$

where t is the irradiation time. Since decomposition of the photosensitizer (photobleaching) is common during PDT, an effective dose (Ψ_{eff}) is specified:

$$\Psi_{eff} = \Theta\left(1 - e^{-\Psi/\Theta}\right), \tag{4}$$

where Θ is the photobleaching parameter.

2.2. Thermal distribution

During PDT, a predominant part of the optical energy is converted to heat through tissue absorption. The thermal distribution in tissue can be expressed as[10]:

$$divgradT - \frac{1}{\chi}\frac{\partial T}{\partial t} - \frac{Q}{\chi}T = -\frac{P_t \alpha^2}{4\pi a \kappa (1+\alpha a)}\left(\frac{a}{r}\right)e^{-\alpha(r-a)}, \quad (5)$$

where T is the temperature rise, Q is the blood flow, α is the optical attenuation coefficient (= $1/\delta$), κ is the thermal conductivity and χ is the thermal diffusivity given by:

$$\chi = \frac{\kappa}{\rho c}, \quad (6)$$

where ρ and c are the mass density and specific heat of blood, respectively.

Since the thermal relaxation time (ca. 5 – 15 min.) is typically an order of magnitude less than the total treatment time, the temperature distribution will be close to the steady-state values for most of the exposure period[10]. Furthermore, since the dimensions of the tissue are much larger than the optical and thermal penetration depths, the medium can be considered as infinitely large in extent. The boundary conditions can thus be specified as zero heat flow at the surface of the applicator and as a finite temperature at infinity. In an infinite medium, the general steady-state solution for a spherical applicator can be written[10]:

$$T = \frac{P_t}{4\pi\kappa\left[1-(\alpha_v/\alpha)^2\right]} \times \frac{1}{r}\left\{\frac{1}{1+\alpha_v a}e^{-\alpha_v(r-a)} - \frac{1}{1+\alpha a}e^{-\alpha(r-a)}\right\}, \quad (7)$$

where α_v is the thermal attenuation coefficient given by:

$$\alpha_v = \frac{1}{\delta_v}, \quad (8)$$

where δ_v is the thermal penetration depth.

3. MATERIALS AND METHODS

3.1 Applicator construction

The applicator was constructed by modifying a standard silicon Foley urine catheter as shown in Figure 1. The distal end was removed and sealed just below the end of the balloon by a transparent silicon plug. The end of the balloon-filling channel, residing in the catheter wall, was also sealed to prevent leakage and balloon deflation. The applicators were gamma sterilized and packaged in two sizes depending on the dimensions of the cavity following tumor resection. The inner diameter of the applicator catheter was 3 or 4 mm depending on the size of the balloon chosen. The balloons could be inflated up to 5 cm in diameter.

3.2 Light Distribution Measurements

Light (λ = 630 nm) from an argon-ion-pumped dye laser was coupled into an optical fiber which was inserted into the balloon applicator. The light delivery fiber has a core diameter of 200 μm and its distal end consists of a 1.4 mm spherical diameter diffuser. The balloon was filled to a diameter of 3 cm with either saline or a 0.1 % Intralipid™ (Kabivitrum, Inc., Clayton, NC) scattering solution. The balloon was immersed in a 2 % Intralipid-filled phantom which simulated the optical scattering characteristics of human brain tissue. Light levels were measured with a 0.8 mm diameter spherical tipped optical detector fiber positioned in contact with the applicator balloon surface. A lock-in detection technique was used to minimize the effect of background noise. Prior to each measurement, light output fluctuations of the laser were monitored and found to be within 3 %.

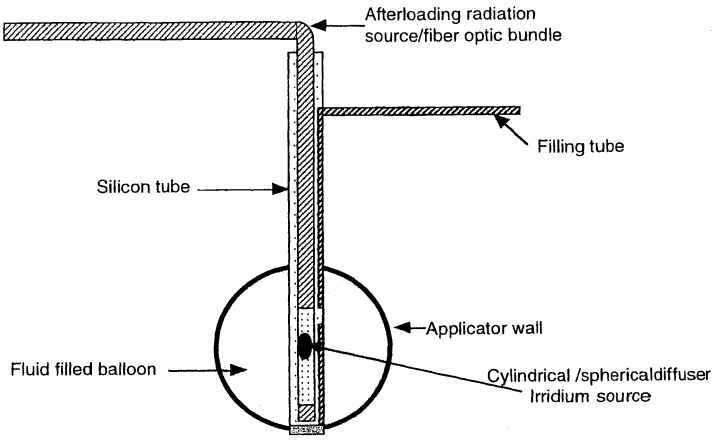

Figure 1. Cross-section illustration of the balloon applicator. It consists of a 6 mm blind ending silicon balloon catheter. The balloon can be inflated through a separate filling channel. Either an ionizing radiation or laser light source can be afterloaded.

4. RESULTS AND DISCUSSION

4.1 Light distribution measurements

Results of the uniformity measurements are shown in Figs. 2a and b. Irradiance was measured as functions of position along the balloon catheter (45° intervals from pole-to-pole), type of catheter-filling fluid (saline, or 0.1% Inrtralipid), and position of source fiber in the applicator (geometric center, or lower pole). Each data point represents the mean of measurements from two applicators.

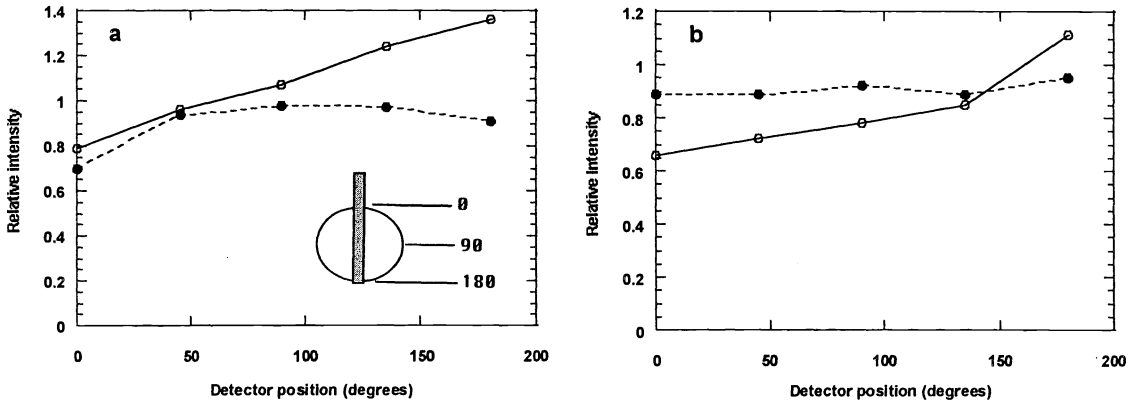

Figure 2. Normalized light output at selected positions along the balloon applicator. The applicator was submerged in a 2% Intralipid scattering solution and measurements were made from pole-to-pole at 45° intervals as shown in the inset. The balloon was filled with saline (a), or a 0.1% Intralipid solution (b). ●: spherical diffuser at balloon center, O: spherical diffuser at bottom of balloon. Data is normalized to the value obtained with the spherical diffusing fiber in the center of the saline-filled balloon, and the detector at the 90° position.

In the case of the saline-filled balloon with the spherical diffuser at the center, the irradiance is uniform to within 5 % except at an angle of 0°. The 30 % decrease in irradiance at this angle is probably due to the inhomogeneity of the irradiance emanating from the spherical diffuser tip. The presence of the fiber prevents emission of light from the diffuser in the backward direction, hence, the amount of light reaching the detector at 0° will be reduced. As shown in Figure 2b, the addition of a scattering solution to the

applicator improves significantly the uniformity of the irradiance. In this case, the irradiance is uniform to within 5 % at all measured locations when the spherical diffuser is positioned in the center of the applicator.

The results suggest that a saline-filled applicator might result in an unacceptable underdose to tissues surrounding the superior aspect of the applicator. Although far from ideal, it is conceivable that the characteristic irradiance from a saline-filled applicator may suit the required light distribution in some patients.

Variations in measured intensity, as a function of source fiber position in the applicator, can be explained in terms of the distance between the spherical source and detector. When the source is placed at the center of the applicator, measured irradiances are independent of detector position since the distance between source and detector is always the same. Conversely, when the source is placed at the bottom of the applicator, measured irradiances increase as the detector is moved towards the bottom of the applicator. The observation of irradiances greater than 100 % for angles in excess of 90° is due simply to the fact that all signals are normalized to the signal obtained for the spherical source fiber located in the center of the saline-filled balloon (detector fiber at 90°). Of clinical relevance is the finding that it is possible to change the light distribution in the resected cavity simply by changing the position of the source within the applicator.

4.2 Treatment time calculations

The time required to deliver a sufficient optical dose to tissues can be determined from knowledge of the fluence rate at the point of interest. Equation (2) was used to estimate fluence rates in brain tissue for three commonly used applicators (Figure 3). The following variables were used in the calculation: a 1 W input power (λ = 630 nm), an optical penetration depth of 3.2 mm[11-13], and a diffusion constant of 5.4 x 10^{10} mm^2s^{-1} [11-13]. Figure 3 illustrates one of the fundamental limitations of PDT, namely the poor penetration of light in biological tissues. For example, the calculations show a decrease in fluence rates of between 3 and 4 orders of magnitude over a tissue depth of 2 cm. Based on the data in Figure 3, treatment times required to deliver a PDT threshold dose of 50 J cm^{-2} are summarized in Table I for three applicator radii (denoted by a). In all cases, an input power of 1 W is assumed.

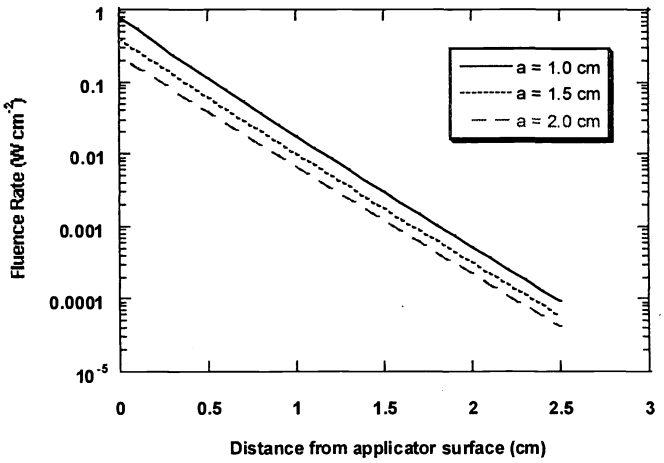

Figure 3. Calculated fluence rates in brain tissue for three different applicators (radii = 1.0, 1.5, and 2.0 cm).

Table I. Time (hours) required to deliver a dose of 50 J cm^{-2}

Depth (cm)	Time (h) a=1.0 cm	a=1.5 cm	a=2.0 cm
1.0	0.8	1.4	2.1
1.5	4.7	7.7	11.5
2.0	26.7	43.0	62.6

The clinical feasibility of treatments lasting for tens of hours must be questioned, even with the use of an indwelling balloon applicator. Furthermore, for realistic input powers of a few Watts, the fluence rates at cm depths in brain tissue are likely too low to evoke a PDT response. For example, it is shown in Figure 3 that, for an input power of 1 W, fluence rates at depths of 2 cm in brain tissue range from 0.2 to 0.5 mW cm^{-2} depending on the applicator diameter. The results of *in vitro* studies in a human glioma spheroid system suggest that a fluence rate of approximately 10 mW cm^{-2} is required for significant PDT response[14]. The input power required for a fluence rate of 10 mW cm^{-2} as a function of depth, is illustrated in Figure 4. Results at specified depths are summarized in Table II.

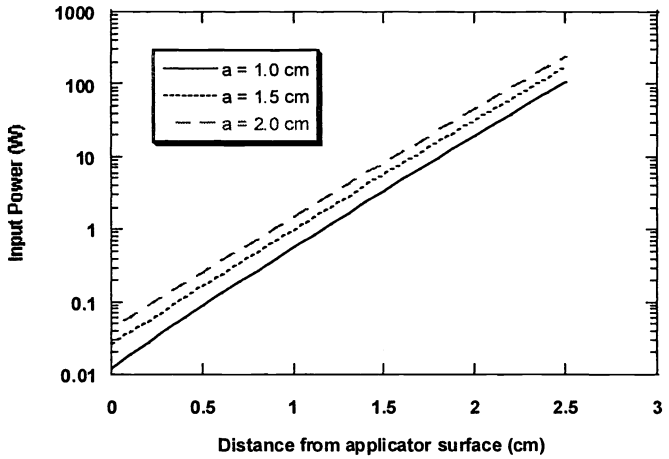

Figure 4. Calculated input powers required for a fluence rate of 10 mW cm^{-2} at various depths in brain tissue.

Table II. Input power required for a fluence rate of 10 mW cm^{-2}

Depth (cm)	Input power (W) a=1.0 cm	a=1.5 cm	a=2.0 cm
1.0	0.6	1.0	1.5
1.5	3.4	5.6	8.3
2.0	19.3	31.0	45.1

The results in Figure 4 (and Table II) show that large input powers are required to obtain threshold fluence rates at cm depths in brain tissue. Although input powers of tens of watts may be possible, the maximum power, and hence the effective treatment depth, will be governed by the thermal damage threshold of brain tissue.

4.3 Thermal distribution calculations

The temperature rise during PDT is dependent on a number of parameters, such as optical absorption and scattering, exposure time, specific heat, thermal conduction, and blood perfusion. The temperature increases rapidly during irradiation and typically reaches a steady-state value after about five minutes of

exposure[15]. This steady-state temperature should be kept below about 45° C in order to avoid hyperthermic reactions[8].

Temperature distributions from various spherical applicators are illustrated in Figure 5. The curves in Figure 5 were calculated from equation (7) using the following values: thermal conductivity of 0.6 W $m^{-1}K^{-1}$ [16], optical penetration depth of 3.2 mm, and thermal penetration depth (white matter) of 10 mm[16]. As expected, the maximum temperature (T_{max}) occurs at the surface of the applicator. Furthermore, for a given input power, T_{max} increases with decreasing applicator diameter. Since T_{max} scales linearly with input power, the input power required for a rise in T_{max} of 8° K (the hyperthermic threshold) can be determined in a relatively straightforward manner. It should be noted that higher input powers are possible if the cavity is cooled, i.e., by the circulation of water through the applicator. For example, calculations show that, for a given input power, a four-fold reduction in T_{max} is possible if the cavity is maintained at ambient temperature, i.e., 37° C[17]. As a result, input powers may be increased by a factor of four simply by cooling the applicator. The input powers resulting in a rise in T_{max} of 8 K, in the presence and absence of cooling, are shown in Table III.

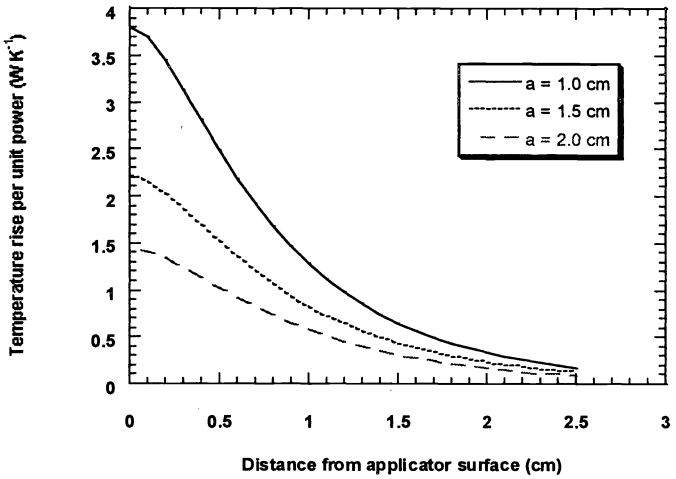

Figure 5. Temperature rise in brain tissue for a 1 W input power. Thermal distributions are shown for three different applicator sizes.

Table III. Input power resulting in a T_{max} rise of 8 K

Applicator Radius (cm)	Input Power (W)	
	No cooling	Cooling
1.0	2.1	8.4
1.5	3.6	14.4
2.0	5.7	22.8

From the curves in Fig. 4, the input powers in Table III correspond to maximum treatment depths of 1.4 and 1.8 cm for the case of no cooling and cooling, respectively. Although it is possible to use very high optical powers if the applicator is cooled, such treatments are not clinically feasible with current laser systems. It should, however, be possible to treat with input powers of a few watts using current state-of-the-art PDT laser systems. It would thus be possible to treat to depths approaching 1.5 cm without cooling the applicator.

This paper addressed only issues related to light delivery in PDT. It is important to realize that, in addition to the light distribution, the overall efficacy of PDT depends in a complex way on factors such as the kinetics of drug uptake, type of drug, cellular localization of the photosensitizer, and tissue oxygenation status. Although, in theory, it may be possible to treat to depths approaching 1.5 cm in brain tissue, the high

fluences associated with such treatments may cause unacceptable normal tissue damage. This is especially true in the case of poorly localizing photosensitizers. It is important to note, however, that, in the high fluence region near the applicator, the optical dose is reduced drastically due to the effects of photobleaching. The effect of photobleaching is illustrated in Fig. 6. The "no-bleaching" and "bleaching" curves were calculated from equations (3) and (4), respectively. An input power of 3.6 W was chosen as this represents the hyperthermic threshold for the 1.5 cm applicator (Table III). A 5000 s radiation time was chosen since this is the time required to deliver a threshold dose of 50 J cm^{-2}, at a dose rate of 10 mW cm^{-2}. It is shown that, in the region close to the applicator where Ψ is much greater than Θ, the bleaching process limits the effective dose to $\Psi_{eff} \cong \Theta$. A bleaching parameter of 50 J cm^{-2} was chosen as this is representative of 5-Aminolevulinic acid[18]. For tissues immediately adjacent to the applicator, photobleaching lowers the optical dose by approximately 2.5 orders of magnitude.

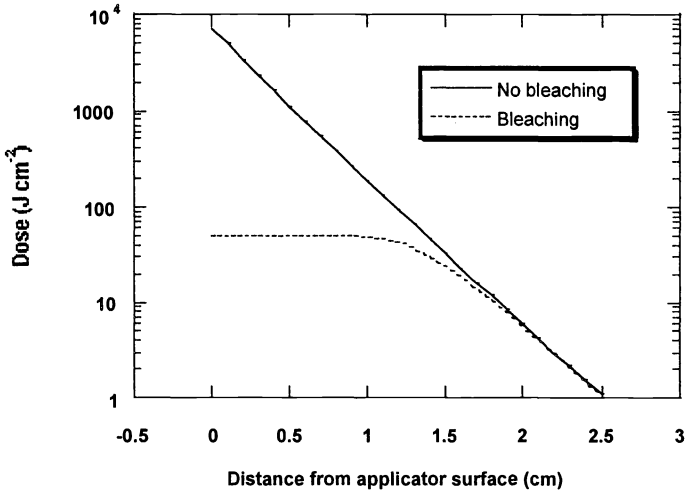

Figure 6. Calculated optical dose and effective optical dose (bleaching) versus distance from the applicator axis. Power = 3.6 W, applicator radius = 1.5 cm, exposure time = 5000 s, bleaching parameter = 50 J cm^{-2}.

The use of a balloon applicator allows for optimization of light delivery in PDT treatments. Since longer treatment times are possible, greater volumes can be irradiated than are currently possible with one-shot intraoperative procedures. Furthermore, since the applicator can be left in the resection cavity for long periods of time (weeks to months), other types of irradiation schemes are possible. This is important in view of recent *in vitro* findings suggesting that light dose fractionation and repeated PDT treatments may be more effective than one-shot procedures[7]. Finally, a vast amount of clinical experience with the applicator suggests that it can be used in PDT treatments over extended periods of time. The balloon applicator is well tolerated by patients – it has already been used for brachytherapy in over 100 patients with few complications.

5. CONCLUSIONS

Measurements of light distribution form a balloon applicator immersed in a brain-simulating phantom, show that it may be used to deliver sufficiently uniform light doses during PDT. The light distribution is uniform to within 5 % when the balloon is filled with a scattering medium. The applicator allows great flexibility in terms of light delivery: treatments are not limited by irradiation times, nor are they limited by thermal damage, especially if the applicator is cooled. Calculations show that it may be possible to deliver threshold light doses to depths of approximately 1.4 cm using balloon applicators of 1.5 cm radius or less. The main drawback of using large applicators is the significant volume of normal brain tissue irradiated. Thus, as is the case with one-shot intraoperative procedures, these types of treatments may be limited by normal tissue complications.

ACKNOWLEDGEMENTS

Steen Madsen is grateful for the support of the UNLV Office of Research and the UNLV Cancer Institute. Henry Hirschberg is grateful for the support of the Norwegian Cancer Society. This work was made possible, in part, through access to the Laser Microbeam and Medical Program (LAMMP) and the Chao Cancer Center Optical Biology Shared Resource at the University of California, Irvine. These facilities are supported by the National Institutes of Health under grants RR-01192 and CA-62203, respectively. In addition, Beckman Laser Institute programmatic support was provided by the Department of Energy (DOE #DE-FG03-91ER61227), and the Office of Naval Research (ONR #N00014-91-C-0134).

REFERENCES

1. M. Salcman, "Epidemiology and factors affecting survival,"in Malignant Cerebral Glioma, M.L.J. Apuzzo, Ed. Amercian Association of Neurological Surgeons, pp. 95-109, 1990.
2. K.E. Wallner, J.H. Galicich, G. Krol, E. Arbit and M.G. Malkin, "Patterns of failure following treatments for glioblastoma multiforme and anaplastic astrocytoma," Int. J. Radiat. Oncol. Biol. Phys. **16,** pp. 1405-09, 1989.
3. R. Ashpole, H. Syndman and A. Bullimore, "A new technique of brachytherapy for malignant glioma with cesium-137," Clin. Oncol. **2,** pp. 333-7, 1990.
4. T.B. Johannesen, K. Watne, K. Lote, J. Norum, R. Hennig, K. Tveraa and H. Hirschberg, "Intracavity fractionated balloon brachytherapy in glioblastoma," Act. Neurochir. (Wien) **141,** pp. 127-33, 1999.
5. P.J. Muller and B.C. Wilson, "Photodynamic therapy: cavitary photoillumination of malignant cerebral tumours using a laser coupled inflatable balloon," Can. J. Neurol. Sci. **12(4),** pp. 371-81, 1985.
6. H. Kostron, A. Obwegeser and R. Jakober, "Photodynamic therapy in neurosurgery: a review," J. Photochem. Photobiol. B: Biol. **36,** pp.157-68, 1996.
7. S. J. Madsen, C.-H. Sun, B.J. Tromberg and H. Hirschberg, "Development of a novel balloon applicator for optimizing light delivery in photodynamic therapy," In preparation.
8. B.J. Tromberg, L.O. Svaasand, M.K. Fehr, S.J. Madsen, P. Wyss, B. Sansone and Y. Tadir, "A mathematical model for light dosimetry in photodynamic destruction of human endometrium," Phys. Med. Biol. **41,** pp. 223-37, 1996.
9. H.J. van Staveren, J.F. Beek, J.W.H. Ramackers, M. Keijzer and W.M. Starr, "Integrating sphere effect in whole bladder wall photodynamic therapy: I. 532 nm vs. 630 nm optical irradiation,"Phys. Med. Biol. **39,** pp. 947-59, 1994.
10. L.O. Svaasand, "Temperature rise during photoirradiation therapy of malignant tumors," Med. Phys. **10(1),** pp. 10-17, 1983.
11. B.C. Wilson and P.J. Muller, "An update on the penetration depth of 630 nm light in normal and malignant human brain tissue *in vivo*," Phys. Med. Biol. **31,** pp. 1295-97, 1986.
12. L.O. Svaasand and R. Ellingson, "Optical properties of human brain," Photochem. Photobiol. **38,** pp. 293-99, 1983.
13. L.O. Svaasand and R. Ellingson, "Optical penetration in human intracranial tumors," Photochem. Photobiol. **41,** 73-76, 1985.
14. S.J. Madsen, C.-H. Sun, B.J. Tromberg, V.P. Wallace and H. Hirschberg, "Photodynamic therapy of human glioma spheroids using 5-aminolevulinic acid," Photochem. Photobiol. **72(1),** pp. 128-34, 2000.
15. L.O. Svaasand, C.J. Gomer and A.E. Profio, "Laser induced hyperthermia of ocular tumors," Appl. Opt. **28, pp.** 2280-7, 1989.
16. L.O. Svaasand, "Thermal distribution from inserted optical fibers," in Optoelectronics in Medicine:Proceedings of the 2nd International Nd:YAG Laser Conference, W. Waidelich and P. Kiefhaber, Eds. Springer-Verlag, pp. 294-301, 1985.
17. L.O. Svaasand, personal communication.
18. E. Hoeydalsvik, "Characterization of the distribution of porphyrins in malignant tumors by fluorescence," M.Sc. Thesis, Division of Physical Electronics, Norwegian Institute of Technology, 1994.